Available online at www.sciencedirect.com
ScienceDirect
Trans. Nonferrous Met. Soc. China 34(2024) 309−321
Transactions of Nonferrous Metals Society of China
www.tnmsc.cn

Precise control and continuous production of β-ammonium tetramolybdate in concentric reactor

Jiang-tao LI[1,2], Yong-jin LUO[1], Zhi-chao LI[1], Zhong-wei ZHAO[1,2], Xu-heng LIU[1], Xing-yu CHEN[1], Li-hua HE[1], Feng-long SUN [1], Ning ZHANG[3]

1. School of Metallurgy and Environment, Central South University, Changsha 410083, China;
2. Key Laboratory of Hunan Province for Metallurgy and Material Processing of Rare Metals, Central South University, Changsha 410083, China;
3. College of Science, Central South University of Forestry and Technology, Changsha 410004, China

Received 2 September 2022; accepted 6 May 2023

Abstract: β-ammonium tetramolybdate [β-$(NH_4)_2Mo_4O_{13}$] was prepared in a concentric structure reactor. The species and microstructure of Mo with the change of solution acidity in the preparation process were investigated. The results showed that the pH of the solution should be controlled below 2.5 to obtain ammonium tetramolybdate crystals. In the acidification process, $NH_3{\cdot}H_2O$ was used to adjust the pH back to about 3.0 to dissolve the fine crystals produced and facilitate the conversion of ammonium heptadmolybdate to ammonium tetramolybdate. Decreasing the soaking time between the $(NH_4)_4Mo_4O_{12}(O_2)_2{\cdot}2H_2O$ crystals and the original liquor was beneficial to obtaining β-$(NH_4)_2Mo_4O_{13}$. Based on the polymerization mechanism of molybdenum, a multi-lattice concentric circle reactor was designed to realize the regional regulation of ammonium molybdate crystallization. High-quality β-$(NH_4)_2Mo_4O_{13}$ was prepared continually by periodically adding HNO_3 solution, ammonia water, and product slurry under specified conditions.
Key words: β-ammonium tetramolybdate; acidification; ionic polymerization; concentric structure reactor

1 Introduction

Molybdenum (Mo) is an important rare metal that is widely used in the iron and steel industry, the military, manufacturing, and the petrochemical fields [1−4]. A strategic study from the Rand Corporation reported Mo as a key raw material that poses a threat to U.S. manufacturing and is included in a list of strategic minerals in China [5,6].

Ammonium tetramolybdate is an intermediate product in molybdenum metallurgy and is the main raw material for the production of molybdenum powders, bars, and other deep-processing products [7,8]. The crystal type, morphology, thermal stability, and purity of ammonium tetramolybdate products directly affect the yield, sintering performance, strength, and toughness of the corresponding molybdenum products [9−11]. In the industry, ammonium tetramolybdate is usually prepared by acidizing ammonium molybdate solution with nitric acid [12−15]. However, due to the complex morphological changes of Mo during the acidification process, the obtained ammonium tetramolybdate crystals often contain small amounts of ammonium trimolybdate and ammonium octadmolybdate. Moreover, ammonium tetramolybdate exists as α and β crystals, and their thermal decomposition characteristics and properties differ significantly [16,17]. For example, α-ammonium tetramolybdate crystals have an uneven particle size and poor thermal stability. When

Corresponding author: Jiang-tao LI, Tel: +86-731-88830476, E-mail: jiangtao-lee@csu.edu.cn;
Ning ZHANG, Tel: +86-731-85623352, E-mail: ningcheung@hotmail.com
DOI: 10.1016/S1003-6326(23)66400-3

α-ammonium tetramolybdate is used as a raw material to produce molybdenum powder, hydrogen does not easily penetrate the particles and the reduction process does not complete, reducing the yield and processing properties of the molybdenum strip. However, *β*-ammonium tetramolybdate has a uniform crystal structure and excellent thermal stability, significantly improving the yield and processing properties of molybdenum strip [18,19]. Therefore, the production of high-quality *β*-ammonium molybdate products to improve the quality of the molybdenum deep processing products is a current research focus of molybdenum smelting enterprises.

In the acid precipitation crystallization of the *β*-ammonium tetramolybdate product, the polymerization of the Mo ion is easily affected by the macroscopic factors of the solution, changing the polymerization morphology of the crystals. Due to the rapid crystallization reaction, the crystallization product usually contains ammonium trimolybdate and ammonium octadmolybdate, while the morphology of the crystals is difficult to control. There is also a crystal transition reaction between *α*-ammonium tetramolybdate and *β*-ammonium tetramolybdate that causes the quality of the *β*-ammonium tetramolybdate products to fluctuate greatly. In recent years, researchers have considered the development of equipment to carefully control the crystallization conditions for the precipitation of *β*-ammonium tetramolybdate to produce high-quality *β*-ammonium tetramolybdate products. For example, an automatic acid settling device was designed to accurately control the timing for the addition of acid, an automatic measurement system for the density of ammonium molybdate was designed to accurately observe the composition changes and crystallization conditions of the solution, and a heating device for the crystallization reactor was designed to control the transformation of *β*-ammonium tetramolybdate in solution [20−22]. The series design can improve the automation and intelligence of ammonium tetramolybdate production and increase the proportion of *β*-ammonium tetramolybdate crystals. However, to obtain higher purity *β*-ammonium tetramolybdate products, it is important to understand the regulation mechanism of *β*-ammonium tetramolybdate crystallization by determining which factors are more closely related.

The changes in Mo ion polymerization morphology during sodium molybdate acidification have been reported prior [23], but most studies only consider the effects of low Mo(VI) concentration or a specific factor on the Mo(VI) species and microstructural changes. Mo(VI) depolymerizes into the molybdyl cation MoO_2^{2+} when the pH of the solution system is about 1−2 [24−27]. In fact, MoO_2^{2+} may not exist in the ammonium molybdate solution when acidized with nitric acid due to the presence of NH_4^+. Therefore, it is often problematic to directly apply the relevant theories obtained under mild conditions to actual processing conditions. Herein, the polymerization mechanism of molybdenum in acidizing the ammonium molybdate solution with nitric acid was investigated. The factors affecting the crystallization morphology were studied to determine the optimal crystallization environment of *β*-ammonium tetramolybdate, providing basic theory and data support for its industrial design. A concentric circle crystallization device was then designed to reasonably segment, regulate, and connect the neutralization, polymerization, nucleation, and crystal growth stages of ammonium molybdate [28]. The device had the advantages of an eco-friendly design, low heat radiation loss, low-power connection, easy-to-automate fine-tuned operation, and continuous production.

2 Experimental

Ammonium molybdate solution (Mo, 120 g/L; pH 7.5) was acidized using HNO_3 solution (3 mol/L) in a 200 mL beaker. The beaker, equipped with an agitator, a thermometer, and an acid burette, was heated using a thermostatically controlled water bath. In each run, a beaker with 100 mL of ammonium molybdate solution was first heated to the required temperature (±0.2 °C). HNO_3 solution was then added at a certain rate, and the change in the pH of the solution was measured in real time. When the pH reached 2.0, $NH_3{\cdot}H_2O$ was added to adjust the pH back to 3.0. When the final pH of the solution reached the specified value, the addition of nitric acid was stopped and the amount of nitric acid added was recorded. The solution was then cooled to room temperature ((29±1) °C), aged for 2 h, and filtered to obtain crystallization products and filtrate. The crystallization products were

finally dried in an oven ((60−80) °C) for about 8 h. To explore the polymerization behavior of molybdenum in the acidic solutions, a series of Mo(VI)–NH_4^+–H^+ solutions were also prepared at room temperature. The components of the corresponding solutions were tabulated, as listed in Table 1.

The Mo concentrations of the solutions were analyzed by inductively coupled plasma optical emission spectroscopy (ICP-OES, IRIS IntrepidII, Thermo Electron Corporation). The morphology and composition of the crystal were analyzed by scanning electron microscopy (SEM) and X-ray diffraction (XRD). The molybdenum content in the crystalline products was determined using the sample dissolution method, and the influence of pH, temperature, concentration, and stirring rate on ammonium tetramolybdate crystallization was studied using the control variable method.

NMR spectra were obtained using an 8.0 mm double-resonance low-frequency probe (JEOL RESONANCE) in a 600 MHz spectrometer (JEOL ECZ600R/S3, Japan) employing a 14.09 T magnet. The ^{95}Mo NMR spectra were collected at 39 MHz and natural abundance with 8192 data points using a 90° pulse. The relaxation delay was fixed at 0.5 s, which is sufficient for the ^{95}Mo nuclei in the distorted octahedral environments found in polymolybdates [23,27]. Due to the relatively low sensitivity of the ^{95}Mo nuclei, up to 9×10^4 scans (~12.5 h) were employed to obtain a high signal-to-noise ratio for the ^{95}Mo NMR spectra depending on the state and composition of the samples. Before the measurements began, the tube was filled with 0.1 mol/L Na_2MoO_4 (containing a few drops of D_2O) and used to calibrate the chemical shifts of ^{95}Mo.

3 Results and discussion

3.1 Polymerization mechanism of molybdenum in acidizing ammonium molybdate solution with nitric acid

Although Na_2MoO_4 solutions acidized by electrodialysis or the addition of H_2SO_4 have been systematically characterized by ^{95}Mo NMR spectra, solutions with the NH_4^+ counterion have been rarely studied in previous literature. However, in relevant solution preparation when acidizing Na^+- or NH_4^+-containing solutions with the same concentration, it was found that the latter was prone to crystallization under slightly acidic conditions. This

Table 1 Mo(VI) concentration, pH, and precipitation occurrence in $(NH_4)_2MoO_4$ solution acidized by HNO_3

No.	Initial Mo(VI) concentration/ (mol·L^{-1})	pH after being acidized with HNO_3	Precipitation	Mo(VI) concentration of supernatant/ (mol·L^{-1})	pH of supernatant
1	0.8	7.48	No	−	−
2	0.8	6.96	No	−	−
3	0.8	6.50	No	−	−
4	0.8	5.98	No	−	−
5	0.8	5.50	No	−	−
6	0.8	4.99	No	−	−
7	0.8	4.50	Precipitation occurs after 5 d in quiescent solution	0.69[a]	4.84[a]
8	0.8	3.99	Precipitation occurs after 1 d in quiescent solution	0.56[a]	4.28[a]
9	0.8	3.48	Precipitation occurs in prepared solution	0.46[a]	3.85[a]
10	0.8	3.04	Precipitation occurs in prepared solution	0.28[a]	3.53[a]
11	0.8	2.44	Precipitation occurs in prepared solution	0.03[b]	2.45[b]

[a]Mo(VI) concentration and pH of supernatants after first and subsequent precipitations; supernatants were observed within 7 d; [b]Mo(VI) concentration and pH of supernatants after first precipitation occurred but subsequent precipitation was not observed within 10 d

indicated that solutions with different counterions may generate different molybdenum solution chemistries. Therefore, the ^{95}Mo NMR spectra of a series of solutions with the NH_4^+ counterion, i.e., $(NH_4)_2MoO_4$ solution, acidized by HNO_3 were also collected (Fig. 1(a)).

In both nearly neutral solutions (pH 7.48 and 6.96), the spectra only displayed a narrow peak (A) at ~0 (Fig. 1(a)), representing the MoO_4^{2-} tetrahedron with a high symmetry configuration. At pH 6.5, besides the narrow peak for MoO_4^{2-}, a new wider signal (B) at ~38×10^{-6} close to the peak previously assigned to $Mo_7O_{24}^{6-}$ was observed, corresponding to the contribution of Mo_I and Mo_{II} (Fig. 2) with at least one terminal oxygen (O_t) in the Mo(VI) octahedral unit [23,27]. This signal (B) gradually increased in intensity upon further acidification, becoming most developed at pH 5.99. In the pH range of 5.98−4.99, an even broader line (C) centered at ~225×10^{-6} was observed, referring to the sole Mo_{III} (Fig. 2) without O_t in the Mo(VI) octahedral unit [23,27]. In contrast, the intensity of the line at ~0 gradually decreased and even disappeared. The above observations suggested that the mononuclear oxoanions were gradually polymerized to heptamolybdate (i.e., $Mo_7O_{24}^{6-}$) in the acidification process.

Further acidification to pH<4.9 caused the solutions to become unstable. The lower the pH was, the more unstable the solutions became (Table 1). The ^{95}Mo NMR spectra of the supernatant and the XRD patterns of the precipitates in these solutions were also measured (Fig. 1). In the initial pH range of 4.5−3.48, the A signal of MoO_4^{2-} (~0) and the B signal assigned to $Mo_7O_{24}^{6-}$ (~38×10^{-6}) were again observed (Fig. 1(a)). For the supernatant of the solution with further acidification, the A signal disappeared and the B signal shifted upfield to ~11×10^{-6} (D) at pH=2.44. This was close to the line previously assigned to $Mo_8O_{26}^{4-}$. However, the

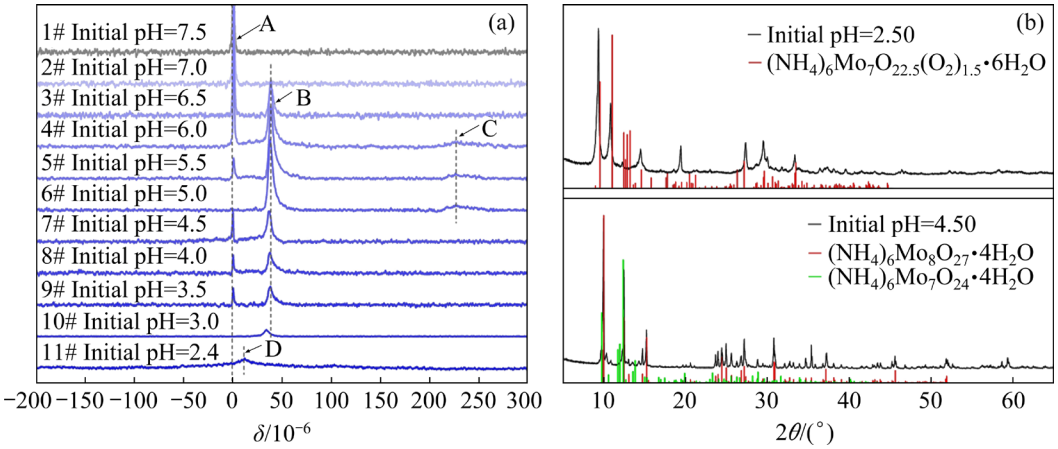

Fig. 1 ^{95}Mo NMR spectra of $(NH_4)_2MoO_4$ solution acidized by HNO_3 at various pH (a), and XRD patterns of precipitate in acidic $(NH_4)_2MoO_4$ solutions (initial pH 4.50 and 2.50) (b)

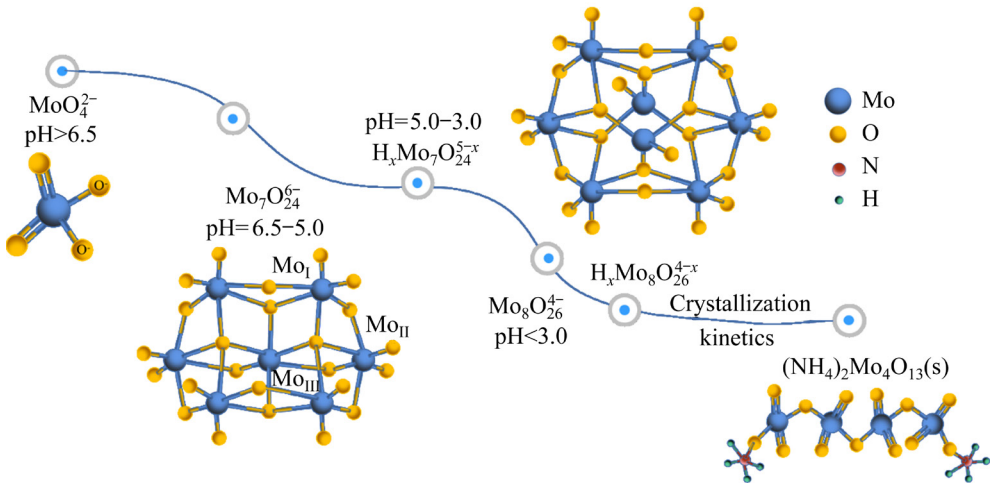

Fig. 2 Polymerization of Mo(VI) in acidic solutions

XRD patterns of the precipitates in the initial pH 4.50 and 2.44 solutions showed that the solids were a mixture of 62% $(NH_4)_6Mo_8O_{27}\cdot 4H_2O$ and 38% $(NH_4)_6Mo_7O_{24}\cdot 4H_2O$ and $(NH_4)_6Mo_7O_{22.5}(O_2)_{1.5}\cdot 6H_2O$ (Fig. 1(b)).

The evolution of Mo(VI) speciation with various pH is summarized in Fig. 2. Although the $Mo_8O_{26}^{4-}$ species dominated in the pH 2.50 solution, the precipitate was mostly $(NH_4)_6Mo_7O_{22.5}(O_2)_{1.5}\cdot 6H_2O$. This suggested that the species found in the original solution was not retained by crystallization. The $Mo_4O_{13}^{2-}$ aqueous species were not formed in the entire pH range. However, after the pH 2.50 suspension was redissolved by adding $NH_3\cdot H_2O$ (pH≈3.0−3.2) and slowly acidized by HNO_3, $(NH_4)_2Mo_4O_{13}$(s) was obtained. A ^{95}Mo NMR signal was observed at ~109.6×10^{-6} with a broad band (not shown), indicating that the formation of $(NH_4)_2Mo_4O_{13}$(s) was depended on complex crystallization kinetics. Based on the analysis results shown in Fig. 1 and Table 1, it was speculated that the polymerization of the molybdenum ion in the pH range of 1.5–6.5 is as described in Eqs. (1)−(4):

pH 6.5−5.0,

$$7MoO_4^{2-}+8H^+=Mo_7O_{24}^{6-}+4H_2O \quad (1)$$

pH 5.0−3.0,

$$Mo_7O_{24}^{6-}+H^+=HMo_7O_{24}^{5-} \quad (2)$$

$$HMo_7O_{24}^{5-}+H^+=H_2Mo_7O_{24}^{4-} \quad (3)$$

pH<3.0,

$$HMo_7O_{24}^{5-}+H^+=H_2Mo_7O_{24}^{4-}$$

$$H_2Mo_7O_{24}^{4-}+4NH_4^++6H_2O=(NH_4)_4H_2Mo_7O_{24}\cdot 6H_2O \quad (4)$$

3.2 Influence factors on preparation of ammonium tetramolybdate by acid precipitation crystallization

In preparation of ammonium tetramolybdate, 100 mL of ammonium molybdate solution (Mo, 120 g/L; pH 7.5) was acidized using HNO_3 solution (3 mol/L) at 30 °C with a stirring speed of 200 r/min. In acidification and crystallization of ammonium tetramolybdate, the solution became turbid when the pH reached 2.5, and a large amount of crystallization occurred at pH 2.0−1.6.

Figure 3 shows the XRD, SEM, and particle size data of ammonium tetramolybdate obtained at the final pH of 1.6 through direct acid precipitation crystallization. The crystallization product was found

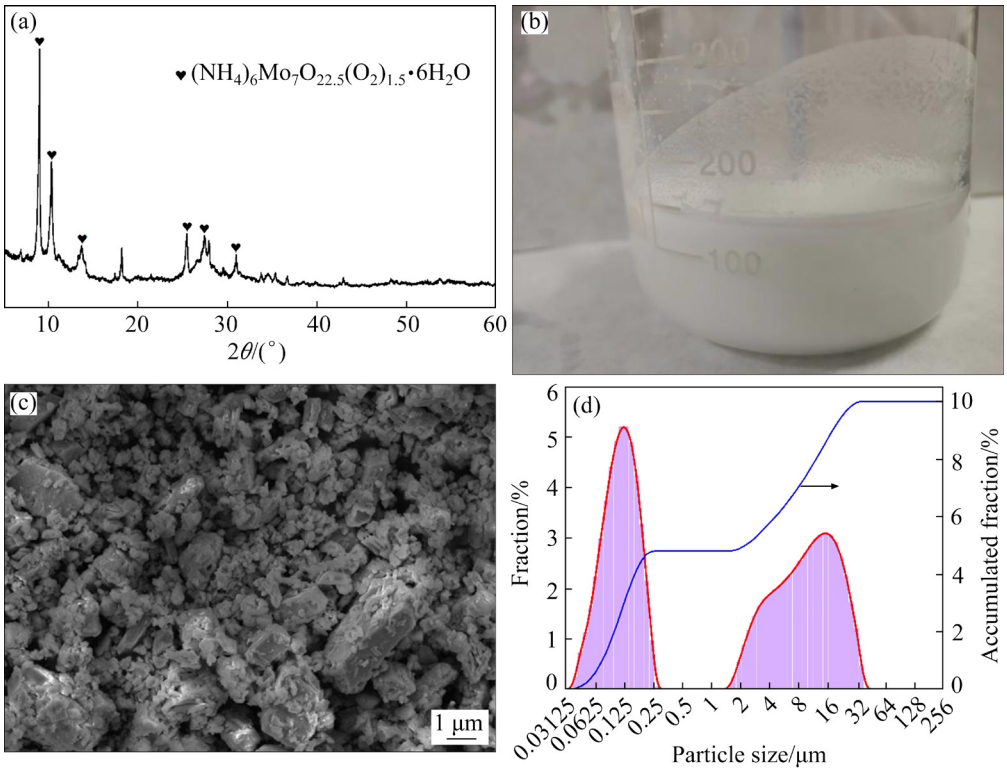

Fig. 3 Characteristics of crystals obtained by direct acid precipitation crystallization: (a) XRD pattern of crystal; (b) Photo of crystallizable solution; (c) SEM image of crystal; (d) Particle size of crystal

to be mainly ammonium heptamolybdate $(NH_4)_6Mo_7O_{22.5}(O_2)_{1.5}\cdot 6H_2O$ (Fig. 3(a)). This inferred that the reaction detailed in Eqs. (1)−(4) mainly took place under these conditions. The obtained crystals were relatively dense, suspended in emulsion in the solution, and difficult to filter thoroughly (Fig. 3(b)). The crystals were not uniform in size, with many tiny and fine crystals smaller than 1 μm (Figs. 3(c, d)).

To prepare the ammonium tetramolybdate product, $NH_3\cdot H_2O$ was added to the solution when the solution pH reached 2.0, and the pH was adjusted back to 3.0. Then, the solution was further acidized by HNO_3 to the final pH of about 2.0. $NH_3\cdot H_2O$ was added to dissolve the fine crystals produced and to facilitate the conversion of ammonium heptadmolybdate to ammonium tetramolybdate, as described in Eqs. (5) and (6):

$$8H_2Mo_7O_{24}^{4-}+4NH_3\cdot H_2O+8H^+= 7Mo_8O_{26}^{4-}+4NH_4^+ +14H_2O \quad (5)$$

$$Mo_8O_{26}^{4-}+4NH_4^+ +4H_2O=2(NH_4)_2Mo_4O_{13}\cdot 2H_2O \quad (6)$$

To prepare an ammonium tetramolybdate product with coarse and uniform crystal morphology, the factors affecting the crystallization morphology were studied to determine the optimal crystallization environment.

3.2.1 Effect of temperature

The crystallization of ammonium molybdate includes the nucleation and crystal growth stages, which are both temperature-controlled processes. The experimental results of the crystallization of Mo at different temperatures are given in Table 2.

At lower temperatures, the effect of temperature on the nucleation rate was dominant. At 30 °C, due to the high nucleation rate, a large number of grains precipitated before they were fully grown and many fine grains attached to the surface of the crystalline products, resulting in their low crystallinity (Fig. 4(a)). No significant characteristic peaks of ammonium tetramolybdate were detected in the XRD patterns shown in Fig. 4(a). When the temperature was increased to 40−60 °C, its influence on the growth rate gradually overtook that of the nucleation rate, which was suitable for the preparation of coarse-grained crystals. At this temperature, the crystal particles gradually became more uniform in size and the morphology normalizes (Figs. 4(b−d)). At temperatures above 60 °C, the proportion of $(NH_4)_2Mo_2O_7$ in the crystallization products increased significantly, while the crystallization products tended to form hard blocks with large crystals and cracks that were

Table 2 Effect of temperature on crystallization efficiency of Mo

Temperature/°C	Nitric acid dosage/mL	Final pH	Mass of crystal/g	Crystallization efficiency of Mo/%
30	52.02	1.29	17.084	86.67
40	52.02	1.43	14.456	74.04
50	51.98	1.56	15.272	78.28
60	52.03	1.63	15.602	81.62
70	52.00	1.81	14.841	77.54
80	52.02	2.56	13.871	70.70

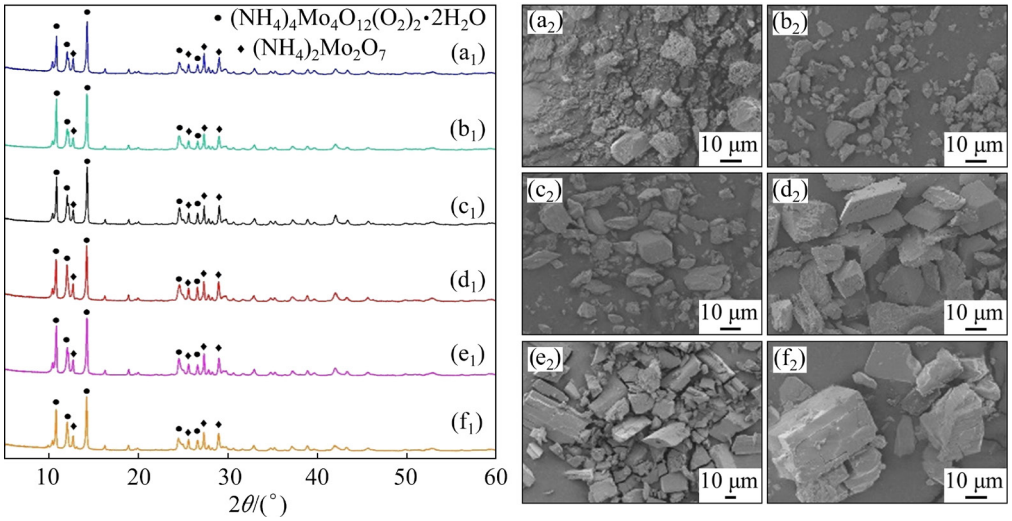

Fig. 4 XRD patterns (a_1−f_1) and SEM images (a_2−f_2) of crystals obtained at different temperatures: (a_1, a_2) 30 °C; (b_1, b_2) 40 °C; (c_1, c_2) 50 °C; (d_1, d_2) 60 °C; (e_1, e_2) 70 °C; (f_1, f_2) 80 °C

not conducive to the subsequent processing and forging of molybdenum materials (Figs. 4(e, f)).

3.2.2 Effect of final pH

The final pH of the ammonium molybdate solution is the most important factor affecting the crystal type of ammonium tetramolybdate. Table 3 shows the effects of the final pH on the crystallization efficiency of Mo under a stirring speed of 200 r/min and a reaction temperature of 60 °C with different dosages of HNO_3. The crystallization efficiency of Mo increased as the final pH decreased, indicating that the solubility of ammonium polymolybdate decreased with the increase of acidity (Table 3). The XRD patterns of the crystals shown in Fig. 5 indicated that the crystallization products were mainly ammonium tetramolybdate [$(NH_4)_4Mo_4O_{12}(O_2)_2{\cdot}2H_2O$] and small amounts of ammonium dimolybdate [$(NH_4)_2Mo_2O_7$]. When the final pH was decreased from 2.50 to 1.60, the diffraction peak intensity of ammonium tetramolybdate increased gradually, indicating that the crystal type and content of ammonium tetramolybdate also increased accordingly. At pH 1.20, the peak strength of ammonium tetramolybdate decreased noticeably. The high acidity led to uneven acidification, the formation of crystal nuclei that could not grow, and crystal particles that were too fine, creating an incomplete crystal structure and greatly reducing the crystallinity of the precipitates. Within the final pH range of 1.60−2.50, the morphology of the crystallization products gradually became normalized as a whole, presenting the massive crystalline product of ammonium tetramolybdate (Fig. 5). At pH 1.20, however, the particle size distribution of the crystallization products was wide, the particles were too fine, and the overall appearance was chaotic, which was not conducive to subsequent processing (Fig. 5(e)).

3.2.3 Effect of Mo concentration

The precipitation rate of the ammonium tetramolybdate crystal is closely related to the supersaturation of the ammonium molybdate solution. At a given temperature and pH, the higher the Mo concentration is, the greater the supersaturation of the solution is, resulting in a higher ammonium tetramolybdate precipitation rate. However, a high concentration of ammonium molybdate is not conducive to the preparation of coarse ammonium tetramolybdate crystals. The effect of Mo concentration on the crystallization efficiency of Mo is given in Table 4. The crystallization efficiency of Mo increased significantly with the Mo concentration of the ammonium molybdate solution. When the ammonium molybdate solution with a Mo concentration of over 120 g/L was treated, the molybdenum crystallization efficiency exceeded 81%. The XRD patterns of the crystals indicated

Table 3 Effect of final pH on crystallization efficiency of Mo

Final pH	Nitric acid dosage/mL	Mass of crystal/g	Crystallization efficiency of Mo/%
2.50	50.96	12.685	65.86
2.25	51.24	14.510	75.02
2.00	51.87	15.767	80.73
1.60	52.03	15.602	81.62
1.20	55.38	17.534	88.21

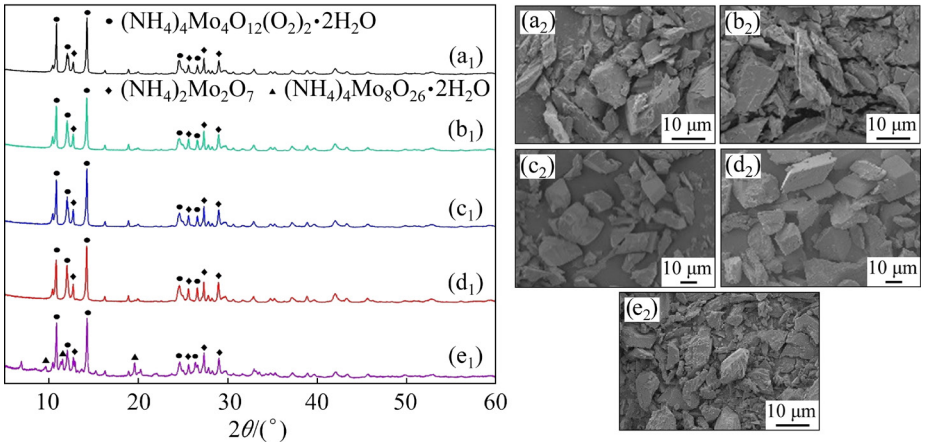

Fig. 5 XRD patterns (a_1−e_1) and SEM images (a_2−e_2) of crystals obtained at different final pH: (a_1, a_2) 2.50; (b_1, b_2) 2.25; (c_1, c_2) 2.00; (d_1, d_2) 1.60; (e_1, e_2) 1.20

Table 4 Effect of Mo concentration on crystallization efficiency of Mo

Mo concentration/ ($g \cdot L^{-1}$)	Nitric acid dosage/mL	Final pH	Mass of crystal/ g	Crystallization efficiency of Mo/%
60	27.32	1.65	5.704	57.98
80	35.88	1.65	9.151	70.19
100	44.22	1.65	12.300	74.54
120	52.03	1.63	15.602	81.62
140	59.65	1.67	18.510	81.92
160	68.20	1.66	21.055	82.71

that the crystallization product was primarily $(NH_4)_4Mo_4O_{12}(O_2)_2 \cdot 2H_2O$ (Fig. 6).

3.2.4 Effect of stirring speed

Mechanical stirring is essential in the acid precipitation crystallization process. Sufficient stirring creates a uniform solution system, preventing uneven acidification to generate fine grains, which is conducive to the preparation of crude ammonium tetramolybdate. At a stirring speed of 140 r/min, the low stirring intensity caused locally overly acidic areas in the solution and crystal nuclei were formed. These were then forced to precipitate and attach to coarse crystals before they were fully grown, causing the overall morphology to become disordered and broadening the particle size distribution (Fig. 7(a)). When the stirring speed was 200 r/min, overall morphology of the crystallization products was regular massive crystals of ammonium tetramolybdate with relatively uniform particle size (Fig. 7(b)). At a speed of 400 r/min, the high stirring intensity resulted in the fragmentation of many crystals and irregular morphology, causing the crystal surface to be covered with many fine grains (Fig. 7(c)).

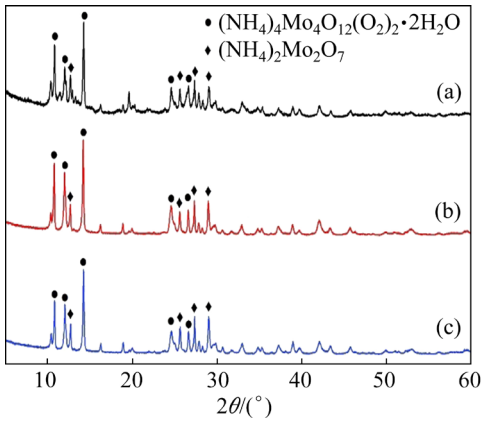

Fig. 6 XRD patterns of crystals obtained from treating ammonium molybdate solutions of different Mo concentrations: (a) 60 g/L; (b) 120 g/L; (c) 160 g/L

The stirring speed has little effect on the Mo crystallization efficiency, remaining at about 80% (Table 5). The XRD patterns of the crystals indicated that the crystallization product was primarily $(NH_4)_4Mo_4O_{12}(O_2)_2 \cdot 2H_2O$ (Fig. 7).

3.2.5 Effect of initial pH

Table 6 details the effect of initial pH on the crystallization efficiency of Mo. The higher the initial pH of ammonium molybdate solution was, the higher the concentration of free NH_3 was. In the acidification of ammonium molybdate solution with nitric acid, more nitric acid was needed to neutralize free NH_3 to produce NH_4^+. Therefore, increasing the concentration of NH_4^+ in the system was beneficial to promoting the crystallization of ammonium tetramolybdate, thus improving the crystallization efficiency of Mo. The XRD patterns of the crystals indicated that the crystallization product was mainly $(NH_4)_4Mo_4O_{12}(O_2)_2 \cdot 2H_2O$ (Fig. 8).

3.2.6 Effect of soaking time

Table 7 showed that increasing the soaking time was conductive to improving the crystallization efficiency of Mo. The ammonium molybdate solution (Mo, 120 g/L; pH 7.5) was acidized using HNO_3 solution (3 mol/L) at 60 °C with a stirring

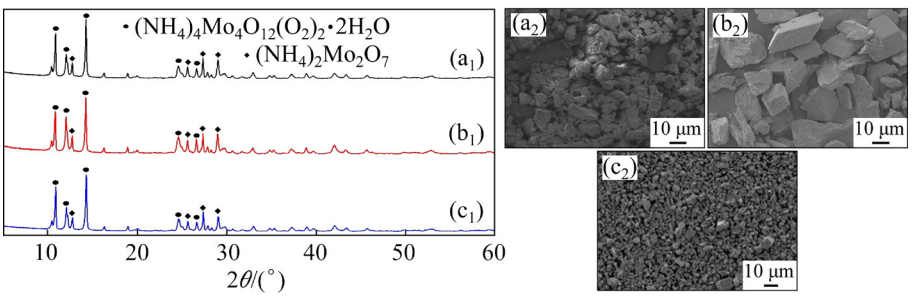

Fig. 7 XRD patterns (a_1−c_1) and SEM images (a_2−c_2) of crystals obtained at different stirring speeds: (a_1, a_2) 140 r/min; (b_1, b_2) 200 r/min; (c_1, c_2) 400 r/min

Table 5 Effect of stirring speed on crystallization efficiency of Mo

Stirring speed/(r·min^{-1})	Nitric acid dosage/mL	Final pH	Mass of crystal/g	Crystallization efficiency of Mo/%
140	51.98	1.69	15.807	79.51
200	52.03	1.63	15.602	81.62
260	52.02	1.53	15.849	80.33
320	51.99	1.59	16.119	80.89
400	52.02	1.56	15.727	80.42

Table 6 Effect of initial pH on crystallization efficiency of Mo

Initial pH	Nitric acid dosage/mL	Final pH	Mass of crystal/g	Crystallization efficiency of Mo/%
7.00	50.77	1.65	15.588	80.72
7.50	52.03	1.63	15.602	81.70
8.00	54.52	1.64	15.931	83.10
8.50	63.16	1.66	16.152	84.23

speed of 200 r/min. When the pH of the solution reached 1.60, the addition of nitric acid was stopped and the solution was filtered to obtain crystallization products and filtrate. The XRD patterns of the crystals shown in Fig. 9(a) indicated that the crystallization product was mainly *β*-ammonium tetramolybdate [$(NH_4)_2O{\cdot}Mo_4O_{12}$]. The morphology of $(NH_4)_2O{\cdot}Mo_4O_{12}$ was a relatively regular long crystal strip, and the size distribution revealed an average particle size of 43.4 μm (Figs. 9(a) and 10(a)).

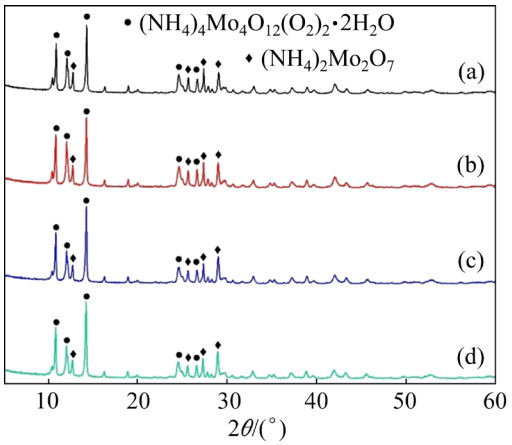

Fig. 8 XRD patterns of crystals obtained at different initial pH: (a) 7.0; (b) 7.5; (c) 8.0; (d) 8.5

Table 7 Effect of soaking time on crystallization efficiency of Mo

Soaking time/h	Nitric acid dosage/mL	Final pH	Mass of crystal/g	Crystallization efficiency of Mo/%
0	52.02	1.60	13.265	68.24
1	52.04	1.62	13.866	70.89
2	51.98	1.61	14.131	72.05
4	52.02	1.61	14.738	74.80
8	52.04	1.60	15.147	76.03

As the holding time increased, the crystal form of ammonium tetramolybdate gradually transformed due to the long contact time between the crystal and the original liquor. When the soaking time was over 4 h, the crystallization product was

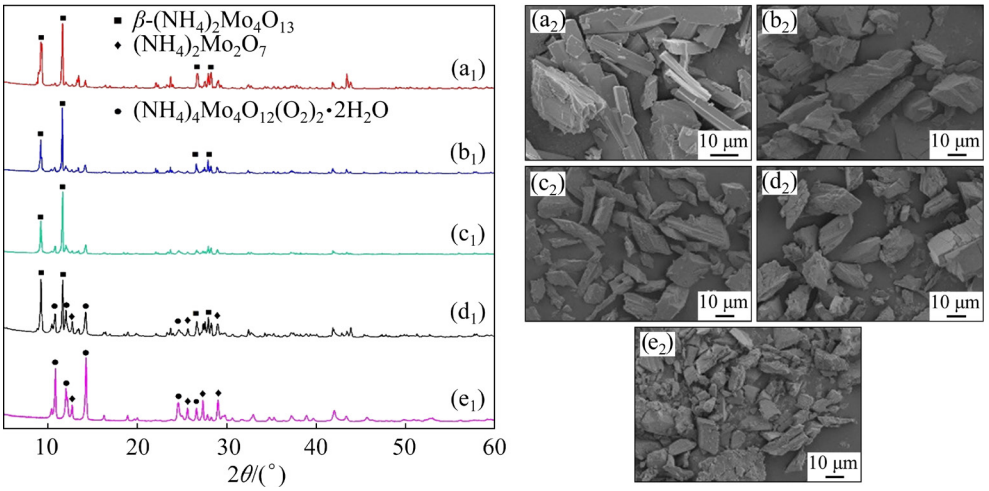

Fig. 9 XRD patterns (a_1−e_1) and SEM images (a_2−e_2) of crystals obtained at different soaking time: (a_1, a_2) 0 h; (b_1, b_2) 1 h; (c_1, c_2) 2 h; (d_1, d_2) 4 h; (e_1, e_2) 8 h

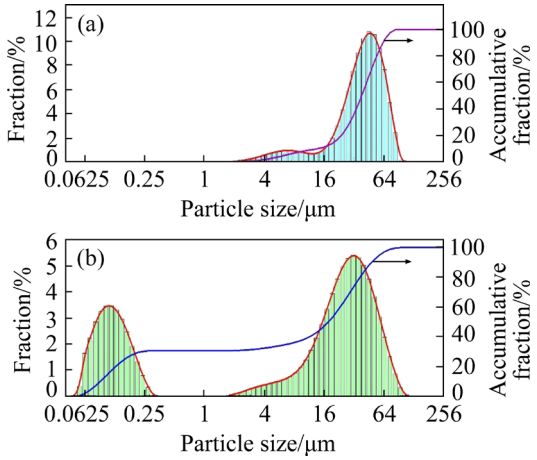

Fig. 10 Particle size distributions of ammonium tetracolybdate at different soaking time: (a) 0 h; (b) 8 h

mainly a mixture of $(NH_4)_4Mo_4O_{12}$-$(O_2)_2{\cdot}2H_2O$ with small amounts of $(NH_4)_2Mo_2O_7$, and the overall morphology was smaller with a wide particle size distribution (Fig. 10(b)).

3.2.7 Effect of adding NH_4^+ to ammonium molybdate solution

According to the Mo polymerization process, the concentration of NH_4^+ in the solution promoted the phase transformation of ammonium tetragolybdate to a certain extent. NH_4NO_3 solution was added to the ammonium molybdate solution (Mo, 120 g/L; pH 7.5), and the mixed solution was acidized using HNO_3 solution (3 mol/L) at 60 °C with a stirring speed of 200 r/min. When the pH of the solution reached 1.60, the addition of nitric acid was stopped and the solution was filtered to obtain the crystallization products and filtrate. The data in Table 8 showed that the crystallization efficiency of molybdenum gradually increased with the amount of added NH_4^+. The XRD patterns of the crystals indicated that the crystallization product was primarily β-ammonium tetramolybdate (Fig. 11(a)). In addition, initial crystallization liquor (containing NH_4NO_3) can be returned for later use, which is beneficial to improving crystallization efficiency of *β*-ammonium tetramolybdate.

Table 8 Effect of adding different concentrations of NH_4^+ on crystallization efficiency of Mo

NH_4^+ concentration/ (mol·L^{-1})	Nitric acid dosage/mL	Final pH	Mass of crystal/g	Crystallization efficiency of Mo/%
0	52.04	1.60	13.265	68.24
0.5	51.98	1.60	13.644	69.98
1	51.86	1.60	13.897	71.05
2	51.72	1.61	14.454	73.80

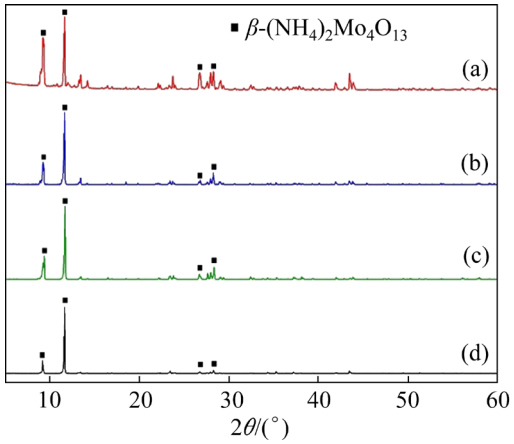

Fig. 11 XRD patterns of crystals obtained by adding NH_4^+ at different concentrations: (a) 0 mol/L; (b) 0.5 mol/L; (c) 1 mol/L; (d) 2 mol/L

3.3 Continuous production of *β*-$(NH_4)_2Mo_4O_{13}$ in concentric reactor

Based on the study of the molybdenum polymerization mechanism (Fig. 2), crystallization of ammonium molybdate can be divided into the neutralization area (pH>6.5, MoO_4^{2-}), the polymerization area (pH=5.0−6.5), the nucleation area (pH=3.0−5.0) and the crystal growth area (pH=1.5−3.0). To continuously prepare a high-quality *β*-$(NH_4)_2Mo_4O_{13}$ product, a concentric reactor was used to segment the above four regions reasonably to achieve the directional regulation of each area. Based on our previous studies in reaction engineering, the concentric structure reactor consisted of six identical single-tank reactors and one circular reactor, each of which was separated by removable vertical separators (Fig. 12).

As shown in Fig. 13, ammonium molybdate feed solution (120 g/L of Mo, pH=7.50) and nitric acid solution (6 mol/L) were pumped into the first single-tank reactor with a peristaltic pump at a constant flow rate. The pH_1 of the solution in the first single-tank reactor was regulated at 6.71 (neutralization area), and the solution then entered the second single-tank reactor. Nitric acid solution was then added to the second single-tank reactor and the pH_3 of the third single-tank reactor was controlled at 3.01 (polymerization area). By adding nitric acid solution to the fourth single-tank reactor, the pH5 of the solution was further reduced to 2.00.

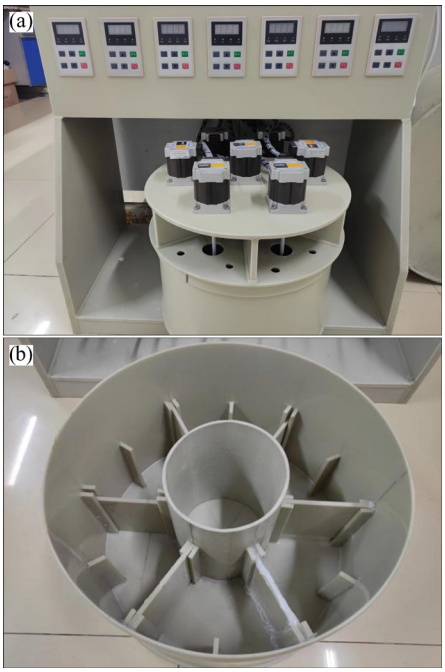

Fig. 12 Concentric reactor

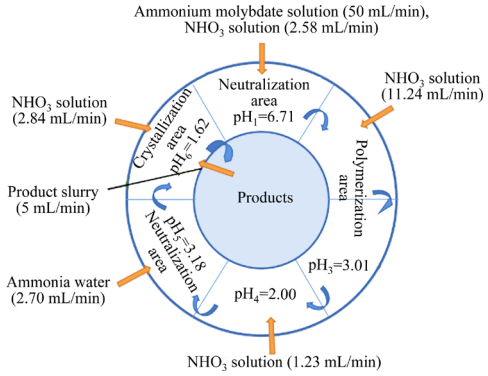

Fig. 13 Continuous crystallization in concentric reactor

Then, ammonia water (6 mol/L) was added to the fifth single-tank reactor to adjust the pH_5 to 3.18. Nitric acid solution was subsequently added to the sixth single-tank reactor to control the pH_6 of the solution at 1.62 (crystallization area) after entering the product area. Finally, using the peristaltic pump to pump the product slurry at a certain flow rate back to the sixth single-tank reactor, the rest was pumped from the system, immediately filtered, and baked at 60−80 °C for 8 h. The temperature of the system was controlled at ~60 °C, and the spectral data of the products are shown in Fig. 14.

The concentric reactor combined operational means of pH regulation, slurry addition, and ammonia solution addition. As determined by semi-quantitative analysis, the main component of the product was β-$(NH_4)_2Mo_4O_{13}$, and its purity was as high as 93.26% after semi-quantitative analysis (Fig. 14). The purity of the crystallized product was greatly improved after precise control at various stages, the addition of seed slurry, and the dissolution of fine crystals with ammonia water. The product morphology was approximately a long strip with a large average particle size of 40−50 μm, which is very suitable for preparing molybdenum strips and molybdenum powder.

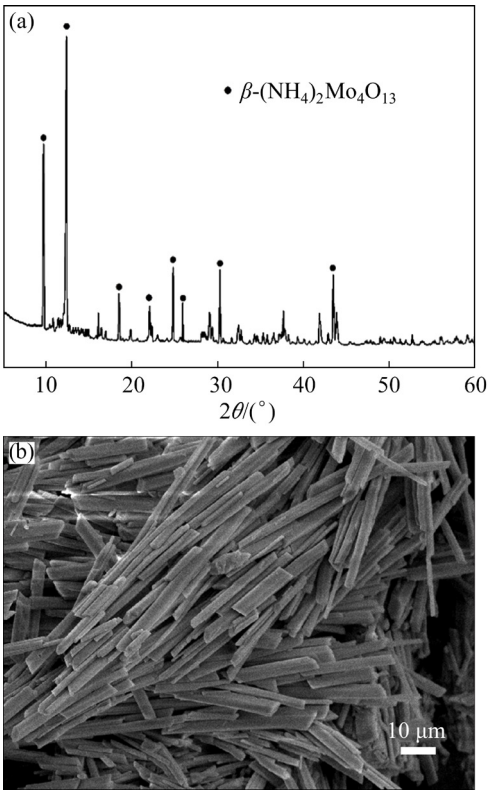

Fig. 14 XRD pattern (a) and SEM image (b) of products

The crystallization efficiency of Mo was about 85%. To further recover Mo from the crystallized mother liquor, the pH of crystallized mother liquor was adjusted to below 1.0, the concentration of molybdenum was reduced to lower than 0.5 g/L, and obtained mixed crystallization of ammonium molybdate molybdenum was redissolved with ammonia water to recrystallize. The secondary crystallization mother liquor (pH value below 1.0) was used to dilute the concentrated nitric acid and then added to the ammonium tetramolybdate crystallization system.

4 Conclusions

(1) The evolution of Mo(VI) speciation with various pH in acidizing ammonium molybdate solution was summarized herein.

(2) The experimental results showed that β-$(NH_4)_2Mo_4O_{13}$ crystals were obtained by controlling the final pH at 1.6 with a reaction temperature of 60 °C, a stirring speed of 140 r/min, and a soaking time of 0 h.

(3) The high-quality β-$(NH_4)_2Mo_4O_{13}$ was prepared in a multi-lattice concentric reactor by periodically adding HNO_3 solution, ammonia water, and product slurry under specific conditions.

CRediT authorship contribution statement

Jiang-tao LI: Ideas, writing original draft, formulation or evolution of overarching research goals and aims; **Yong-jin LUO:** Writing original draft, scrub data and maintain research data for initial use and later reuse; **Zhi-chao LI:** Writing original draft, scrub data and maintain research data for initial use and later reuse; **Zhong-wei ZHAO:** Management and coordination responsibility for the research activity planning and execution; **Xu-heng LIU:** Provision of study materials, reagents, materials, patients, laboratory samples, animals, instrumentation, computing resources, or other analysis tools; **Xing-yu CHEN:** Investigation, Writing − Original draft; L**i-hua HE:** Editing; **Feng-long SUN:** Editing; **Ning ZHANG:** Writing original draft, scrub data and maintain research data for polymerization mechanism of molybdenum in acidizing the ammonium molybdate solution with nitric acid.

Declaration of competing interest

The authors declare that they have no known competing financial interests or personal relationships that could have appeared to influence the work reported in this paper.

Acknowledgments

This work was financially supported by the National Natural Science Foundation of China (Nos. 52174340, 51704338), the Basic Science Center of the National Natural Science Foundation of China (No. 72088101), and the National Key Research and Development Project of China (No. 2022YFC2904505).

References

[1] LASHEEN T A, EL-AHMADY M E, HASSIB H B, HELAL A S. Molybdenum metallurgy review: Hydrometallurgical routes to recovery of molybdenum from ores and mineral raw materials [J]. Mineral Processing & Extractive Metallurgy Review, 2015, 36(3): 145−173.

[2] ZHOU Qiu-sheng, YUN Wei-tao, XI Jun-tao, LI Xiao-bin, QI Tian-gui, LIU Gui-hua, PENG Zhi-hong. Molybdenite−limestone oxidizing roasting followed by calcine leaching with ammonium carbonate solution [J]. Transactions of Nonferrous Metals Society of China, 2017, 27: 1618−1626.

[3] LI Xiao-bin, WU Tao, ZHOU Qiu-sheng, QI Tian-gui, PENG Zhi-hong, LIU Gui-hua. Kinetics of oxidation roasting of molybdenite with different particle sizes [J]. Transactions of Nonferrous Metals Society of China, 2021, 31: 842−852.

[4] LI Zhi-hua, LU Jin, WU Sheng-xi, ZHANG Gui-qing, GUAN Wen-juan, ZENG Li, LI Qing-gang, CAO Zuo-ying. Sustainable extraction and complete separation of tungsten from ammonium molybdate solution by primary amine N1923 [J]. ACS Sustainable Chemistry & Engineering, 2020, 8: 6914−6923.

[5] RICHARD S, JAMES T B, BRIAN G C, DAVID L A, KYLE B. Critical materials−Present danger to U.S. manufacturing [M]. Rand Corporation Publisher, Santa Monica, 2013: 15−40.

[6] LI Wen-chang, LI Jian-wei, XIE Gui-qing, ZHANG Xiang-fei, LIU Hong. Critical minerals in China: Current status, research focus and resource strategic analysis [J]. Earth Science Frontiers, 2022, 29(1): 1−13. (in Chinese)

[7] MAI Geng-peng, ZHANG Chao, SONG Jian-xun, CHE Yu-si, HE Ji-lin. Preparation of highly uniform molybdenum powder by the short-process reduction of molybdenum trioxide with hydrogen [J]. International Journal of Refractory Metals & Hard Materials, 2021, 100: 105644.

[8] GU Si-yong, QIN Ming-li, ZHANG Hou-an, MA Ji-dong, QU Xuan-hui. Preparation of Mo nanopowders through hydrogen reduction of a combustion synthesized foam-like MoO_2 precursor [J]. International Journal of Refractory Metals & Hard Materials, 2018, 76: 90−98.

[9] YANG Li-qun, LI Xiao-bin, QI Tian-gui, LIU Gui-hua, PENG Zhi-hong, ZHOU Qiu-sheng. Direct synthesis of pure ammonium molybdates from ammonium tetramolybdate and ammonium bicarbonate [J]. ACS Sustainable Chemistry & Engineering, 2020, 8: 18237−18244.

[10] CAO Hua-zhen, TONG Cheng-jian, ZHANG Hui-bin, ZHENG Guo-qu. Mechanism of MoO_2 electrodeposition from ammonium molybdate solution [J]. Transactions of Nonferrous Metals Society of China, 2019, 29: 1744−1752.

[11] YANG Li-qun. Technical and theoretical research on the preparation of ammonium polymolybdates by in-situ re-dissolution and crystallization method [D]. Changsha: Central South University, 2021. (in Chinese)

[12] ZHANG Meng-ping, LIU Chen-hui, ZHU Xiong-jin, XIONG Hua-bin, ZHANG Li-bo, GAO Ji-yun, LIU Man-hong. Preparation of ammonium molybdate by oxidation roasting of molybdenum concentrate: A comparison of microwave roasting and conventional roasting [J]. Chemical Engineering and Processing−Process Intensification, 2021, 167: 108550.

[13] ARACENA A, SANINO A, JEREZ O. Dissolution kinetics of molybdite in KOH media at different temperatures [J]. Transactions of Nonferrous Metals Society of China, 2018,

28: 177−185.
[14] QIN Qing-wei, LIU Zhen-wei, CHEN Tie-jun, HUANG Zi-li, YANG Jian-hong, HAN Wei. Study for preparation of industrial ammonium molybdate from low grade molybdenum concentrate [M]//Rare Metal Technology. San Diego, California, USA: TMS, 2017: 265−276.
[15] CAO Zhan-fang, ZHONG Hong, QIU Zhao-hui, LIU Guang-yi, ZHANG Wen-xuan. A novel technology for molybdenum extraction from molybdenite concentrate [J]. Hydrometallurgy, 2009, 99: 2−6.
[16] ZHANG Jing. Regulated preparation of β-ammonium tetramolybdate and its effect on molybdenum powder [D]. Zhengzhou: Zhengzhou University, 2021. (in Chinese)
[17] LIU Wu-sheng. Application of β-ammonium tetramolybdate [J]. China Molybdenum Industry, 2001, 25: 58−61. (in Chinese)
[18] LI Xi. Study and production of β-ammonium tetramolybdate [J]. China Chemical Trade, 2020, 15: 244−246. (in Chinese)
[19] WU Zheng-ping, YIN Zhou-lan, CHEN Qi-yuan, ZHANG Ping-min. The preparation of β-ammonium tetramolybdate and the crystallization process [J]. Journal of Central South University of Technology: Science and Technology, 2001, 32(2): 135−138. (in Chinese)
[20] GAO Xian-li, DENG Li-nan. An automatic acid settling control device for preparing ammonium molybdate: CN Patent, ZL201821793289.7 [P]. 2019−09−17.
[21] YI Jian, AN Wei, LUO Shi-hua, LIU Jin-rui. An automatic measurement system for specific gravity of ammonium molybdate: CN Patent, ZL201820292451.0 [P]. 2018−10−26.
[22] XU Shuang, ZHOU Wen-min, LENG Huai-en, LI Zhi-yong, LIU Jian. A production method and production system for β-ammonium tetramolybdate: CN Patent, ZL201110360531.8 [P]. 2013−10−09.
[23] MAKSIMOBSKAYA R I, MAKSIMOV G M. ^{95}Mo and ^{17}O NMR studies of aqueous molybdate solutions [J]. Inorganic Chemistry, 2007, 46: 3688−3695.
[24] WANG Ming-yu, JIANG Chang-jun, WANG Xue-wen, XIAN Peng-fei, WANG Hua-guang, YANG Yang. Existing form of Mo(VI) in acidic sulfate solution [J]. Rare Metals, 2015, 34: 1−5.
[25] MOFFAT J B. Metal-oxygen clusters: the surface and catalytic properties of heteropoly oxometalates [M]. Kluwer, New York, 2001: 20−50.
[26] ZHANG Ning, HE Shan, LI Yong-li, ZHOU Ju-qiu, ZENG De-wen, ZHAO Zhong-wei, YAN Jun, ZENG Jian-rong, HEFTER G. Spectroscopic study of the behavior of Mo(VI) and W(VI) polyanions in sulfuric-phosphoric acid mixtures [J]. Inorganic Chemistry, 2021, 60: 17565−17578.
[27] ZHANG Ning, KONIGSBERGER E, DUAN Si-qi, KE Lin, YI Hai-bo, ZENG De-wen, ZHAO Zhong-wei, HEFTER G. Nature of monomeric molybdenum(VI) cations in acid solutions using theoretical calculations and Raman spectroscopy [J]. Journal of Physical Chemistry B, 2019, 123: 3304−3311.
[28] LI Jiang-tao, LI Zhi-chao, ZHAO Zhong-wei, LIU Xu-heng, CHEN Xing-yu, HE Li-hua, SUN Feng-long, LUO Yongjin, CUI Mu-ye. Method for crystallization of beta-ammonium tetramolybdate: US Patent, 17992949 [P]. 2022−11−23.

同心圆式反应器中精确调控和连续制备 β-四钼酸铵

李江涛[1,2]，罗勇进[1]，李志超[1]，赵中伟[1,2]，刘旭恒[1]，陈星宇[1]，何利华[1]，孙丰龙[1]，张 宁[3]

1. 中南大学 冶金与环境学院，长沙 410083；
2. 中南大学 稀有金属冶金与材料制备湖南省重点实验室，长沙 410083；
3. 中南林业科技大学 理学院，长沙 410004

摘 要：采用同心圆式反应器制备 β-四钼酸铵，研究制备过程中 Mo 离子聚合形态和微观结构受溶液酸度影响的变化规律。结果表明，将溶液的 pH 值控制在 2.5 以下可以得到四钼酸铵晶体；采用 $NH_3·H_2O$ 将溶液 pH 值调回至 3.0 有利于细粒钼酸铵结晶的溶解，并促进七钼酸铵向四钼酸铵结晶的转变；降低$(NH_4)_4Mo_4O_{12}(O_2)_2·2H_2O$ 晶体与结晶母液的接触时间有利于获得 β-$(NH_4)_2Mo_4O_{13}$ 结晶。基于钼的聚合机理，设计多个格区的同心圆反应器，实现钼酸铵结晶的分区域调控。通过调控硝酸、氨水和含晶种的母液在各格区中加入的位置和时机，可制备出优质的 β-$(NH_4)_2Mo_4O_{13}$ 结晶。

关键词：β-四钼酸铵；酸化；离子聚合；同心圆式反应器

(Edited by Bing YANG)